Supplemental Figure S1

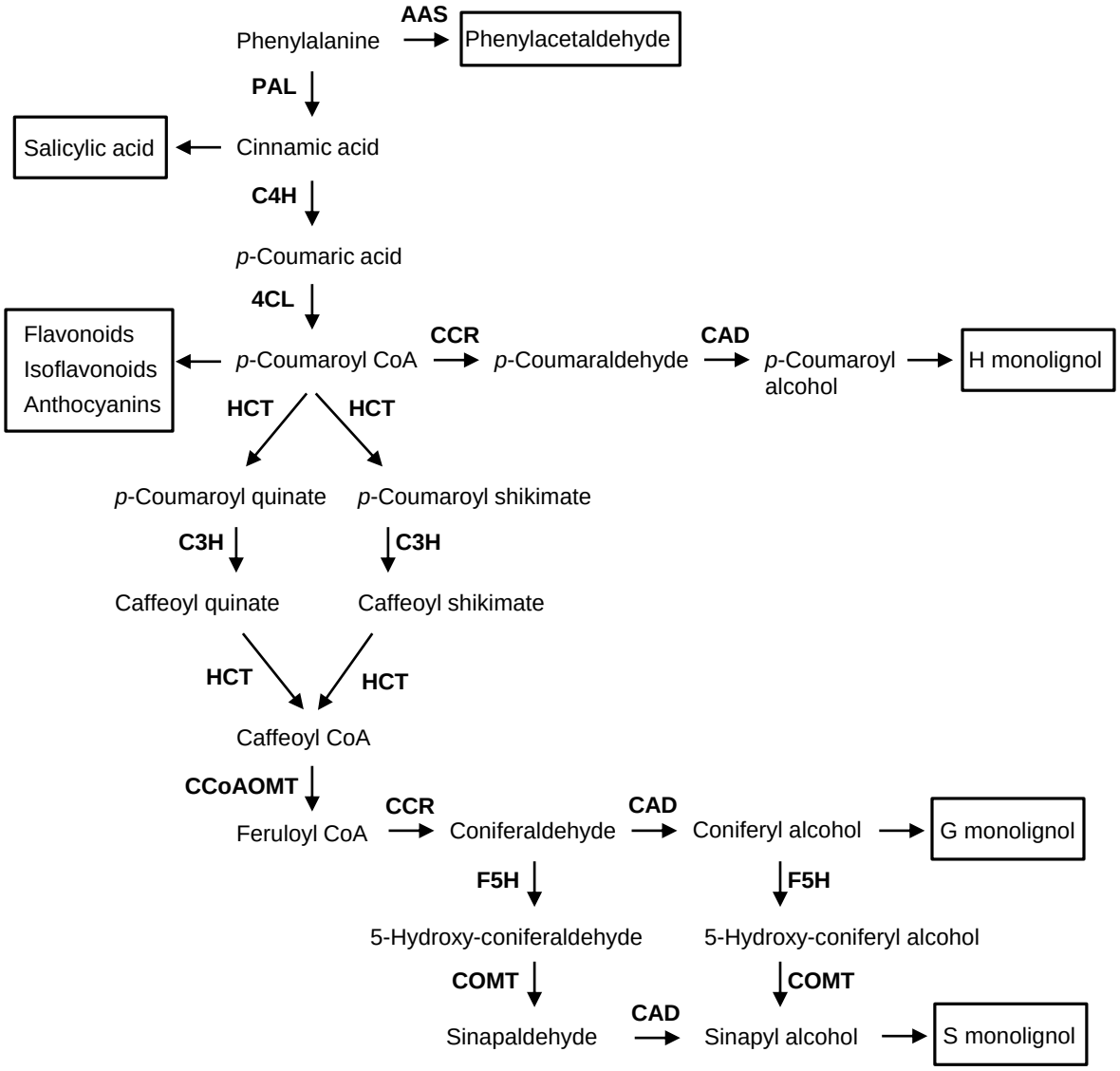

Supplemental Figure S1. The phenylpropanoid pathway, modified according to prevous studies (Hoffmann et al., 2004; Li et al., 2010). 4CL, 4-hydroxycinnamoyl-CoA ligase; AAS, aromatic aldehyde synthase; C3H, *p*-coumarate 3-hydroxylase; C4H, cinnamate 4-hydroxylase; CAD, cinnamyl-alcohol dehydrogenase; CCoAOMT, caffeoyl-CoA *O*-methyltransferase; CCR, cinnamoyl-CoA reductase; COMT, caffeic/5-hydroxyferulic acid *O*-methyltransferase; F5H, ferulate 5-hydroxylase; HCT, hydroxycinnamoyltransferase; PAL, phenylalanine ammonia lyase.

Supplemental Figure S2

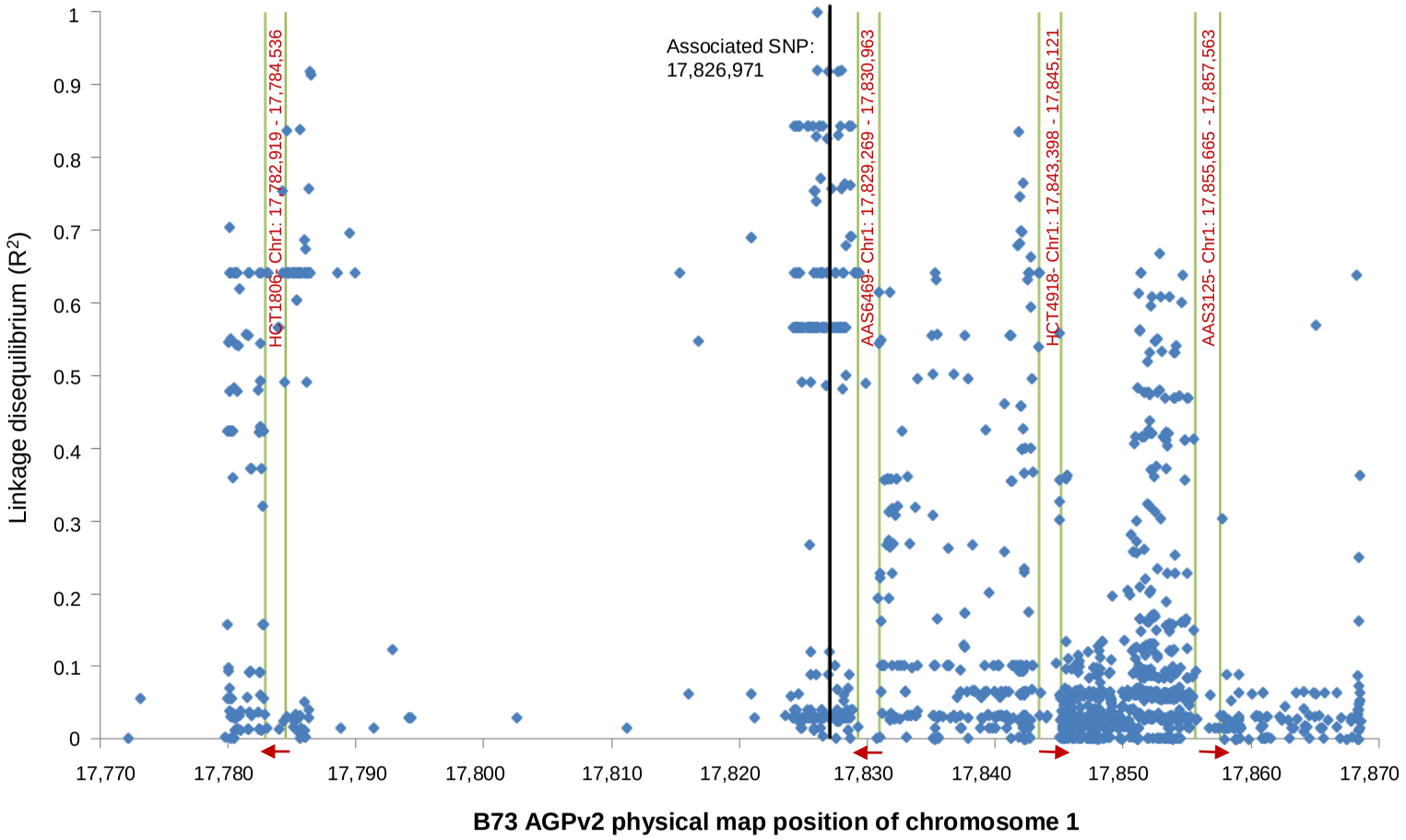

Supplemental Figure S2. Linkage disequilibrium between the SNP at chromosome 1, 17,826,971 bp, indicated by a black line, and adjacent SNPs. The X-axis indicates the position on chromosome 1 of each SNP in base-pairs. The four annotated genes in the region are indicated and bounded by orange lines. Their transcriptional directions (5' to 3') are indicated below the X-axis. The Y-axis indicates levels of linkage disequilibrium measured as an R^2 value with a maximum value of 1.

Supplemental Figure S3

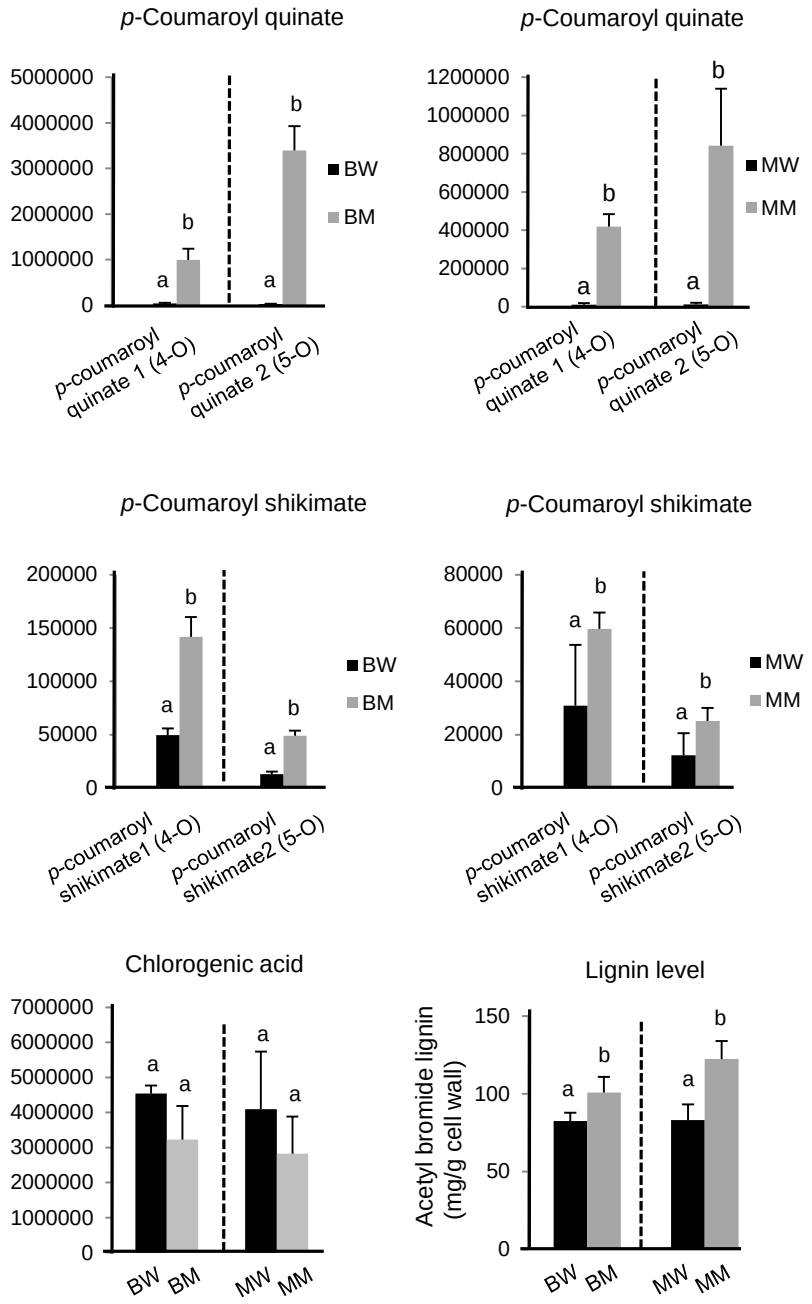

Supplemental Figure S3. Differential accumulation of hydroxycinnamic acid esters and lignin between isolines with or without Rp1-D21. The contents of *p*-coumaroyl quinate, *p*-coumaroyl shikimate, chlorogenic acid and lignin were measured from the isolines with or without Rp1-D21 in B73 × H95 and Mo17 × H95 backgrounds. Significant difference between samples was labeled by different letters. BW: wild type in B73 × H95; BM: *Rp1-D21* mutant in B73 × H95; MW: wild type in Mo17 × H95; MM: *Rp1-D21* mutant in Mo17 × H95. Values are average of four biological replicates and the error bars represent standard deviation. The Y-axis in the metabolite charts is peak area.

Supplemental Figure S4

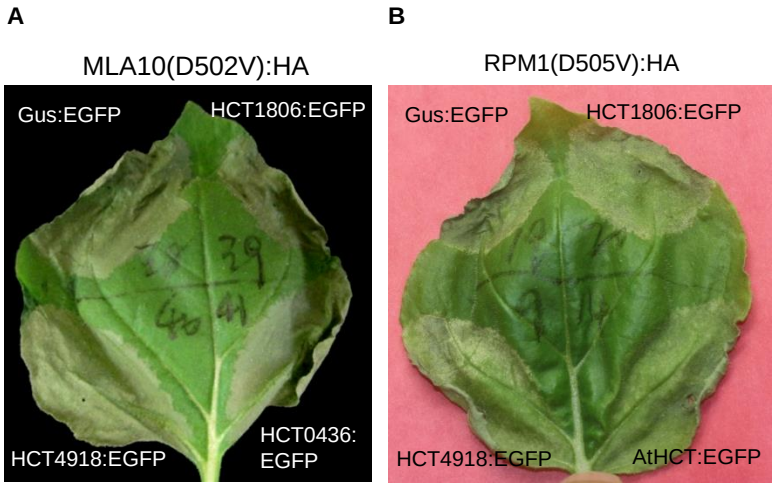

Supplemental Figure S4. HCT1806 and HCT4918 did not suppress MLA10(D502V)- and RPM1(D505V)-induced HR in *N. benthamiana*. **A,** The HR phenotype resulting from the transient co-expression of HCT1806, HCT4918, HCT0436 or Gus with MLA10(D502V). **B,** The HR phenotype resulting from transient co-expression of HCT1806, HCT4918, AtHCT or Gus with RPM1(D505V). Agrobacterium carrying MLA10(D502V) or RPM1(D505V) was diluted to a final concentration of OD_{600}=0.2, while agrobacterium carrying EGFP-tagged HCT construct was diluted to a final concentration of OD_{600}=0.4 plus p19 with OD_{600}=0.2. The pictures were taken at 2 days after inoculation. The experiments were repeated three times with the same results.

Supplemental Figure S5

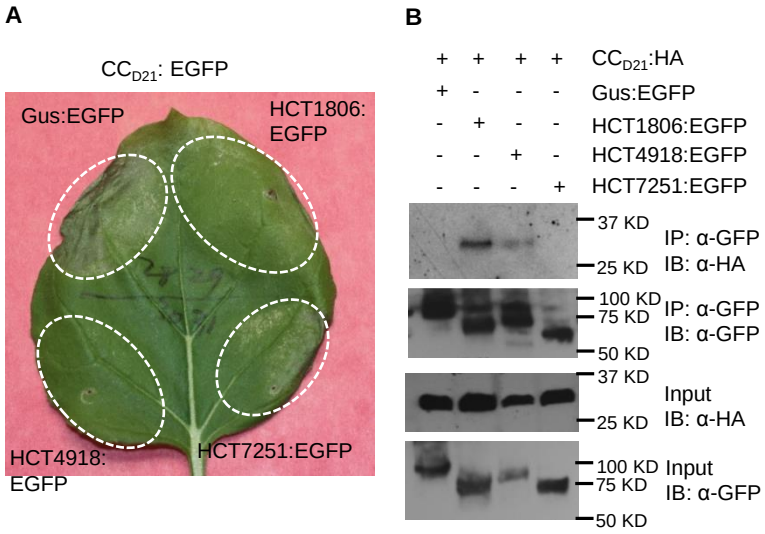

Supplemental Figure S5. Investigating the function of HCT1806/HCT4918/HCT7251 in CC_{D21}-induced HR. **A,** HCT1806 and HCT4918 suppressed CC_{D21}-induced HR in *N. benthamiana*. CC_{D21}:EGFP was transiently co-expressed with EGFP-tagged HCT1806, HCT4918, HCT7251 or Gus, and a representative HR picture was taken at 2 days after inoculation. **B,** Investigating the interactions between CC_{D21} and HCT1806/HCT4918/HCT7251 by co-immunoprecipitation (Co-IP) assay. EGFP- and 3×HA-tagged constructs were transiently co-expressed in *N. benthamiana* and samples were collected at 30 hpi for Co-IP assay. Protein extracts were immunoprecipitated (IP) by anti-GFP (α-GFP) microbeads and detected (Immunblotted-IB) by anti-GFP and anti-HA (α-HA) antibodies. The experiments were repeated three times with the same results.